The alignment tool is then inserted and positioned so that the beam from the auxiliary laser intersects the center of the beamsplitter. While the corner cube will retroreflect any incident beam, collinearity of the incident and reflected beams requires that the alignment laser and corner cube are positioned so that the transmitted beam strikes the apex of the corner cube. The optimal position in practice is readily found by observing the increased brightness due to the scattering of the laser beam when it strikes the apex. The angular alignment of the corner cube can be checked by observing coincidence between the weakly reflected beam from the front surface of the corner cube and the intense, internally reflected beam on the alignment laser. Finally, the prism table is adjusted until the axis of the collinear beams is made coincident with that of the auxiliary laser. The tool thereafter acts as a reference for checking the internal alignment of the spectrometer.

Alignment to the telescope and detector is straightforward. The more intense beam, specifically chosen for this purpose, is directed to the center of the telescope's secondary mirror (the condition for optical alignment) by adjusting the input optics of the spectrometer. In our application, the spectrometer has two input ports (one points to the astronomical object, and the other to an adjacent region of the sky, at similar airmass, to provide cancellation of atmospheric emission) and the corresponding laser spots must overlap on the secondary mirror. Alignment to the detector similarly is accomplished by adjusting the final mirror in the spectrometer so that the exiting laser spot strikes the center of the detector optics. The alignment tool then is removed from the beam and the infrared signal obtained from an astronomical calibration source (*e.g.*, Mars or Jupiter) is maximized by making fine adjustments to this mirror position and the detector itself. Finally, the tool is reinserted and the laser spot position on the mirror and the detector optics is recorded for future reference.

Conclusion

A simple optical alignment tool has been developed that produces two accurately parallel, but oppositely directed, laser beams for the alignment of a spectrometer with an astronomical telescope and detector. The tool can be remotely and accurately inserted into the spectrometer at any time to aid alignment, and has been found to be particularly useful to periodically check this alignment.

Reference

1. D. A. Naylor, G. J. Tompkins, T. A. Clark, and G. R. Davis, in ASP Conference Series **41**, Calgary, Alberta, Canada, June 1992, *Astronomical Infrared Spectroscopy*, S. Kwok, ed. (1993), p. 405.

A Novel Method for Measuring the Vertical Birefringence of Optical Disk Substrates

By M. Mansuripur and Yung-Chieh Hsieh, Optical Sciences Center, The University of Arizona, Tucson, Arizona 85721

Abstract

We describe a simple method of measuring vertical birefringence over the entire surface of an optical disk substrate. Our design consists of a linearly polarized He-Ne laser (1-2 mW) and a CCD camera interfaced to a computer. The measurement is non-intrusive, easy to set up, and needs only a few seconds to collect the data and plot a map of vertical birefringence over the surface area of the disk. The system described here is potentially useful as a quality-control tool in substrate manufacturing environments.

Recently, optical disk substrates have been produced reliably and inexpensively by the injection molding of polycarbonate (PC) plastics. One disadvantage of PC substrates is their birefringence: the injection-compression molding process produces disks in which the refractive indices n_r, n_t, and n_z along the radial, tangential, and vertical directions are slightly different from one another. At the operating wavelength of $\lambda = 780$ nm, for instance, typical values of these indices are:

$$n_r = 1.581$$
$$\Delta n_{\parallel} = n_r - n_t = 2 \times 10^{-5}$$
$$\Delta n_{\perp} = n_r - n_z = 5 \times 10^{-4}$$

$\Delta n_{\parallel}$, known as the lateral (or in-plane) birefringence causes a phase shift between the components of polarization parallel and perpendicular to the tracks; this is particularly troublesome for magneto-optical disk readout, where the substrate-induced phase shift interferes with the readout signal derived from the magneto-optical Kerr effect. The vertical birefringence, $\Delta n_{\perp}$, causes problems because the read/write laser beam is generally focused on the storage medium through the substrate at fairly large numerical apertures (NA ≥ 0.5). Depending on their state of polarization, the various oblique rays going through the substrate will be delayed differently by the vertical birefringence. This could induce a certain amount of astigmatism in the beam, which would in turn disturb the magneto-optical read signal, or enhance the feedthrough problem (*i.e.*, the cross-talk be-

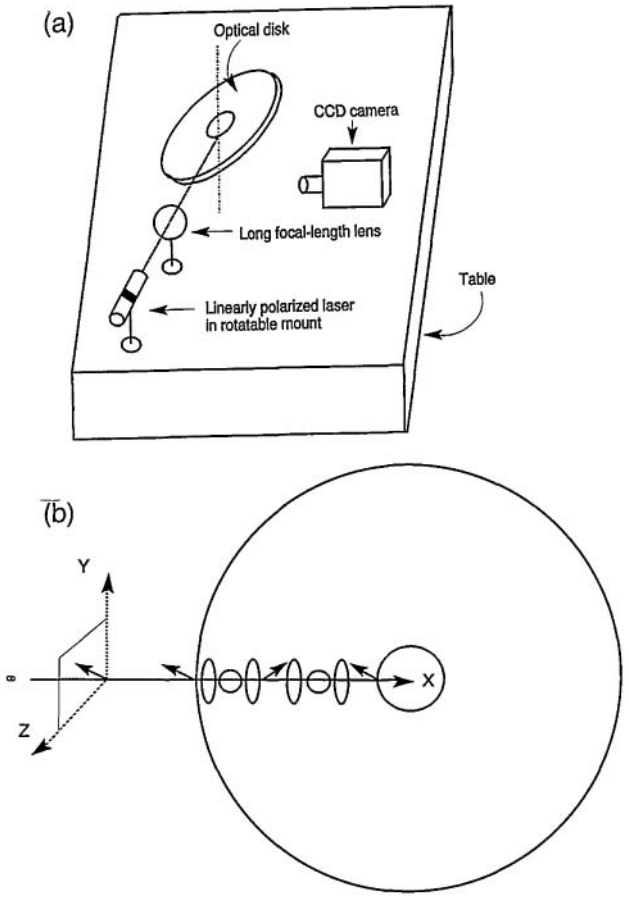

FIGURE 1. (a) Schematic diagram of the birefringence measurement system. (b) The changing state of polarization of the beam as it propagates through the substrate. Only one complete oscillation is shown; however, polycarbonate substrates have a fairly large vertical birefringence, resulting in an oscillation period of ≈1 mm.

tween focusing and tracking servo channels), or produce a number of other undesirable effects.[1-4]

Advantages

Several authors have reported on the measurements of birefringence (both lateral and vertical) using various ellipsometric techniques.[5-8] These measurements tend to be elaborate, time-consuming, and confined to probing one small area at a time. Most often, these measurements are also intrusive in that they either slice and destroy the substrate, or render it unsuitable for further processing by the application of index-matching fluid during the measurement. In contrast to the existing methods, the technique of measuring vertical birefringence described here is fast, nonintrusive, and applicable to the entire area of the disk. These features can be useful for quality control in the substrate manufacturing process.

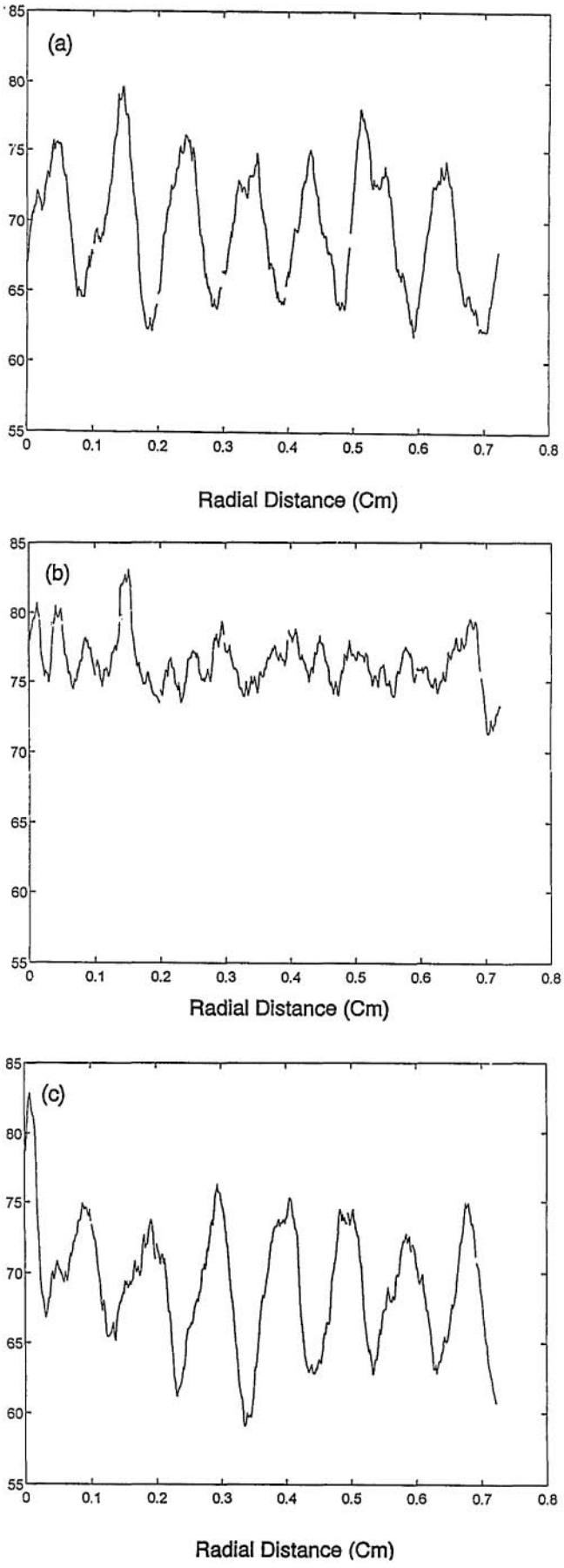

FIGURE 2 (right). Intensity of the scattered light along one radius of the disk. In (a) the incident polarization is parallel to the table. In (b) the polarization is at 45° to the table, namely, parallel to the plane of the disk. In (c) the incident polarization is perpendicular to the table. In both (a) and (c) the period of oscillations is approximately 1.05 mm.

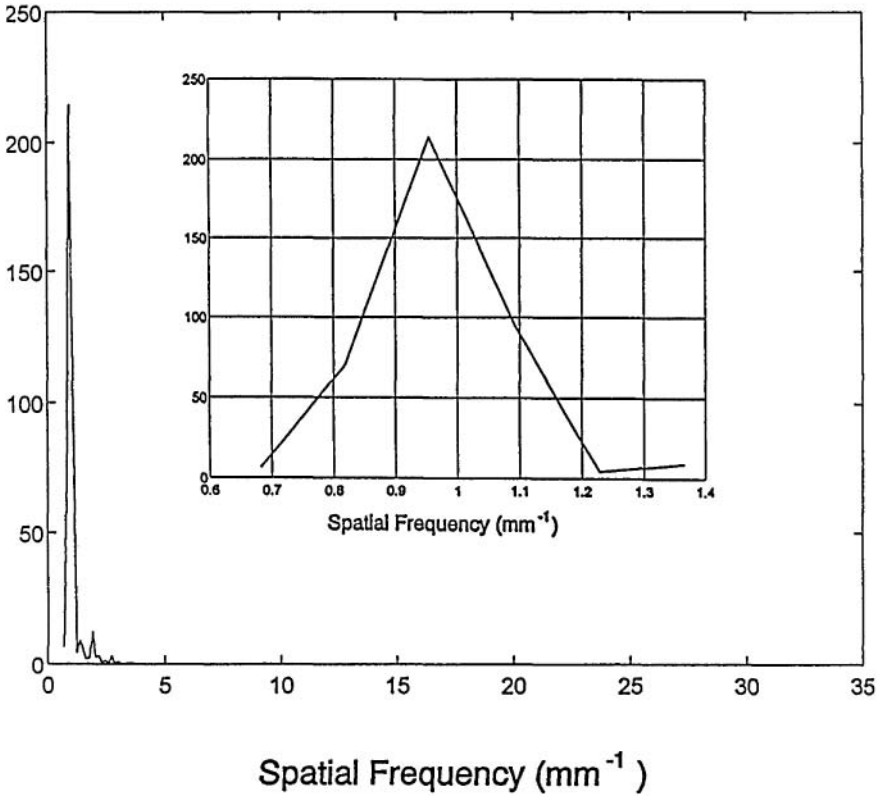

FIGURE 3. Fourier spectrum of the light intensity distribution depicted in Figure 2(a). Peak at $f = 0.95$ mm^{-1} corresponds to periodic oscillations of polarization as the beam propagates along a disk radius. Inset is a magnified view of the peak.

System Description

Our birefringence measuring system is schematically depicted in Figure 1(a). The 1 mW red He-Ne laser is linearly polarized and can be rotated in its mount, thus producing a beam with an arbitrary angle between its polarization direction and the plane of the table (the reference plane). The beam enters the substrate from the edge and propagates within the disk along the radial direction. Scattering of the beam by the substrate inhomogeneities will render the beam visible to the CCD camera. The disk is oriented at 45° to the table; thus, if the incident polarization happens to be either parallel or perpendicular to the plane of the disk, it will propagate without a change in its state of polarization. However, when the incident polarization makes a 45° angle with the plane of the disk (*i.e.*, polarization either parallel or perpendicular to the table), then the beam will undergo periodic conversions along its path from linear, to elliptical, to circular, to elliptical, and back to linear polarization. These various states of the beam are depicted in Figure 1(b).

The scattered rays that reach the CCD camera are mainly parallel to the table. Where the polarization inside the disk is linear and horizontal, scattered photons traveling parallel to the table are at a minimum; at such points the light reaching the camera is fairly weak. Where the polarization inside the disk is perpendicular to the table, the horizontally scattered photons are abundant, and the CCD will pick up a strong signal. We thus expect to see a periodic pattern of intensity along the path of the beam.

Figure 2 shows plots of scattered light intensity along the optical path as picked up by the camera. In (a) the incident polarization is parallel to the table, giving rise to strong periodic variations of the scattered light. In (b) the incident polarization is at 45° to the table (*i.e.*, parallel to the plane of the disk); the periodic variations are absent in this case. In (c), where the polarization is perpendicular to the table, the periodic intensity pattern returns. The period of these oscillations L is related to the vertical birefringence $\Delta n_\perp$ of the substrate through the following formula:

$$L = \frac{\lambda}{\Delta n_\perp}$$

At $\lambda = 633$ nm and with a measured period of $L \simeq 1.05$ mm, the above formula yields $\Delta n_\perp \simeq 6 \times 10^{-4}$, which is consistent with other measurements of the same substrate.[8]

The period of oscillations can be derived fairly accurately from a Fourier spectrum of the intensity patterns of Figure 2. Figure 3 shows the spectrum of the signal displayed in Fig. 2(a); the noise now appears as a constant background, but the signal manifests itself as the sharp peak at the (spatial) frequency of 0.95 mm^{-1}. The width of this peak is a measure of the variations of birefringence over the radial range covered by the measurement (provided, of course, that the measurement range is wide enough to render the truncation errors negligible). The inset to Figure 3 shows a magnified view of the peak, revealing its full width at half maximum (FWHM) to be around 0.23 mm^{-1}. If the radial range over which the data was collected had been sufficiently wide, this width would have corresponded to a fluctuation of $\pm 0.7 \times 10^{-4}$ in the measured value of $\Delta n_\perp$.

Acknowledgment

We thank Hong Fu for help in setting up the experiment, as well as participating in many illuminating discussions. The work reported here has been supported by a grant from the Advanced Research Projects Agency (ARPA) through the National Storage Industries Consortium (NSIC).

References

1. D. Treves and D. S. Bloomberg, "Effect of birefringence on optical memory systems," in *Optical Mass Data Storage II*, R. P. Freeses, A. A. Jamberdino, and M. deHaan, eds., Proc. SPIE **695,** 262-269 (1986).
2. A. B. Marchant, "Retardation effects in magneto-optic readout," in *Optical Mass Data Storage II*, R. P. Freeses, A. A. Jamberdino, and M. deHaan, eds., Proc. SPIE **695,** 270–276 (1986).
3. W. A. Challener and T. A. Rinehart, "Jones matrix analysis of magneto-optical media and read-back systems," Appl. Opt. **26,** 3974-3980 (1987).
4. A. Takahashi *et al.*, "Influence of birefringence on the signal quality of magneto-optical disks using polycarbonate substrates," Appl. Opt. **27,** 2863-2866 (1988).

5. A. Skumanich, "Substrate birefringence in coated optical disks," J. Magn. Soc. Jpn. **17,** Supplement S1, 237-240 (1993).
6. S. Shirouzu *et al.*, "Refractive index ellipsoids of a polycarbonate magneto-optical memory disk substrate," Jpn. J. Appl. Phys. **28,** 797-800 (1989).
7. J. E. Hayden and S. D. Jacobs, "Automated spatially scanning ellipsometer for retardation measurements of transparent materials," Appl. Opt. **32,** 6256–6263 (1993).
8. H. Fu, S. Sugaya, J. K. Erwin, and M. Mansuripur, "Measurement of birefringence for optical recording disk substrates," Appl. Opt. **33,** 1938–1949 (1994).

Three-channel Homodyne Interferometer

By V. Greco, C. Iemmi, S. Ledesma, G. Molesini, and F. Quercioli, Istituto Nazionale di Ottica, Florence 50125, Italy, and M. Varasi, ALENIA, Rome 00131, Italy

Abstract
A three-channel homodyne interferometer based on a structured delay plate is described. Detection and data acquisition are performed with standard optoelectronics in a PC environment. The device, which is used as a displacement sensor, features sub-nanometric sensitivity.

Two-channel homodyne interferometers have long been used successfully as simple displacement sensors up to $\lambda/8$ sensitivity.[1] Early approaches were based on two signals in close quadrature, using TTL circuitry and Boolean logic to perform bidirectional fringe counting. The availability of fast and accurate A/D converters made possible improving the resolution by proper digitization of the signals and data processing in a PC environment. Such signals have the general form:

$$I = A + B\cos\phi, \tag{1}$$

where A is the mean intensity, B the modulation amplitude, and ϕ the phase to be detected. Two-channel interferometers work at $\pi/2$ nominal phase lag. However, two measurements are not sufficient to solve for ϕ.

Multiphase interferometers have recently been introduced, increasing the number of measuring channels and achieving ultra-high sensitivity.[2] A Twyman-Green configuration is reported here, where three signals at $2\pi/3$ nominal phase lag are made available (Fig. 1). The interferometer makes use of corner cube reflectors in both arms, and includes a structured delay plate that, in double pass, produces the desired phase relationships (Fig. 2). The three detectors are placed at convenient locations in the interference pattern, so that the signals are obtained,

$$\begin{aligned} I_1 &= A_1 + B_1\cos(\phi + \epsilon_1),\\ I_2 &= A_2 + B_2\cos\left(\phi + \frac{2\pi}{3} + \epsilon_2\right),\\ I_3 &= A_3 + B_3\cos\left(\phi + 2\frac{2\pi}{3} + \epsilon_3\right) \end{aligned} \tag{2}$$

being ϵ_1, ϵ_2, ϵ_3 phase errors. As with phase-stepped interferometry,[3] the quantities:

$$\begin{aligned} x &= 2I_1 - I_2 - I_3,\\ y &= \sqrt{3}(I_3 - I_2) \end{aligned} \tag{3}$$

are evaluated. With simple mathematics it can be shown that x,y reduce to the parametric coordinates of an ellipse according to:

$$\begin{aligned} x &= a + b\cos\phi,\\ y &= c + d\sin(\phi + \epsilon), \end{aligned} \tag{4}$$

where a, b, c, d, ϵ are constants that depend on A_i, B_i, ϵ_i.

The phase ϕ is then expressed in explicit form:

$$\tan\phi = \frac{b}{(x-a)\cos\epsilon}\left(\frac{y-c}{d} - \frac{x-a}{b}\sin\epsilon\right). \tag{5}$$

The phase is defined modulo 2π, and unwrapping procedures have to be implemented as with similar approaches.[3]

For our laboratory setup, the delay plate has been obtained with thin film deposition technology. Two SiO_2 step layers have been coated on a glass substrate according to the geometry of Figure 2; the thickness was monitored to

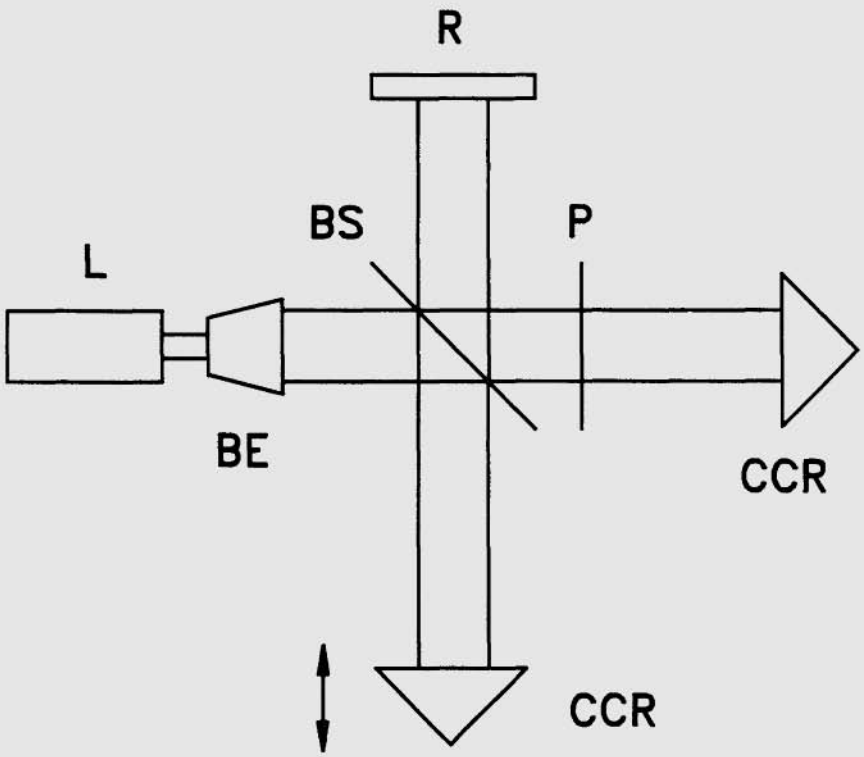

FIGURE 1. Three-channel Twyman-Green interferometer. L, laser; BE, beam expander; BS, beam splitter; P, optical delay plate; CCR, corner cube reflector; R, three detector arrangement.